Technium Vol. 24, pp.1-10 (2024)
ISSN: 2668-778X
www.techniumscience.com

The design of a labyrinth seal to replace the centrifugal compressor of a turbojet, for transforming the turbojet into a turboexpander

Theodor Mihnea SIRBU[1], Diana Andreea NAN[2], Calin PROFIR[3], Ioana Cristina MANDREANU[4], Mara AMARIUTEI[5], Cosmin Petru SUCIU[6], Alexandru HANK[7], Bogdan NAVLIGU[8], Ramona Manuela STANCIUC[9], Iulian VLADUCA[10,*]

[1, 3, 6, 7, 8, 9, 10]Romanian Research and Development Institute for Gas Turbines COMOTI, Bucharest, Romania, theodor.sirbu@comopti.ro
[2, 4, 5]Faculty of Aerospace Engineering, National University of Science and Technology Politehnica Bucharest
*Correspondig author: Iulian VLADUCA, iulian.vladuca@comoti.ro

Abstract. In the last 10 years, the development of microturboreactors has experienced an exponential evolution. They have recently gained interest due to the significantly higher power output, which is primarily achieved by expanding the speed ranges of the key components, namely the compressor and the turbine. Also, the development of bearings with ceramic balls (also known as hybrid bearings) at high speeds of 80,000 rpm in the case of the present work, brings a challenge regarding the design of the main components (compressor + turbine), which must withstand very high centrifugal force demands that increase with the diameter of the component, especially for the turbine that faces additional thermal stress, respectively reaching a creep limit. From a technical standpoint, at relatively low power consumption, the challenges have been addressed for turbojets with a modest thrust of 40 daN (90 lbf), making such turbojets available at relatively low prices [1]. In the present work it is proposed to modify a 40 daN (90 lbf) turbojet and transform it into an axial turboexpander [2] capable of theoretically gearing an electric generator of 132/160 kVA (177/215 HP), by means of a gear reducer taking into account the losses related to the gear reducer and the electric generator. The proposed transformation has commercial values, such axial turboexpanders are able to work in electricity generation mode having the availability of a relatively low source of compressed air of maximum 10 bar (150 PSI).

Keywords. labyrinth, micro-turbojet, turbo-expander.

1. Introduction

The small turbojets of 40 daN (90lbf), have been developed in the last years especially for drone propulsion, being used for civilian and military purposes. In Romania, there is also a great interest for developing such applications with land and airspace monitoring drones and for many other civil and military applications. The present work has a special application regarding the production of energy where acces to compressed air sources is easily available, allowing the development of powers clearly superior to those developed by the free expansion of compressed air with ordinary turbines. The power is produced by the combustion of fuel. The power generation will be relatively high for its small dimension, and lends itself to local in situ applications.

Technium Vol. 24, pp.1-10 (2024)
ISSN: 2668-778X
www.techniumscience.com

In figure 1 is shown a such small turbojet complete equiped, with its calculation points marked [3]. The turbojet from the figure presents a small radial compressor and a small axial turbine, that are the subjects for modifications in the present paper.

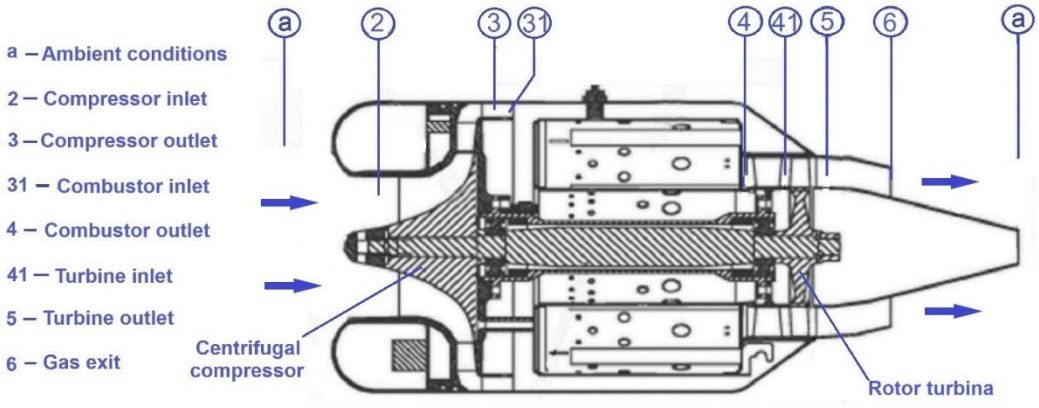

Fig. 1. Small 40 daN (90 lbf) turbojet

2. Labyrinth design

In the design of centrifugal compressors operating at high rotational speeds, a compression ratio of approximately $\pi c \sim 4.5$ can be achieved [4]. As a result, the pressure at point 31, at the entrance to the combustion chamber, will be around $p31 = 4.5$ bar, considering the losses in the intake nozzle. Using an external source of compressed air allows the removal of the centrifugal compressor, which can be replaced with a labyrinth seal. This labyrinth seal would not only serve its primary function but also counteract the axial force generated by the turbine, thereby balancing the net axial force of the entire assembly.

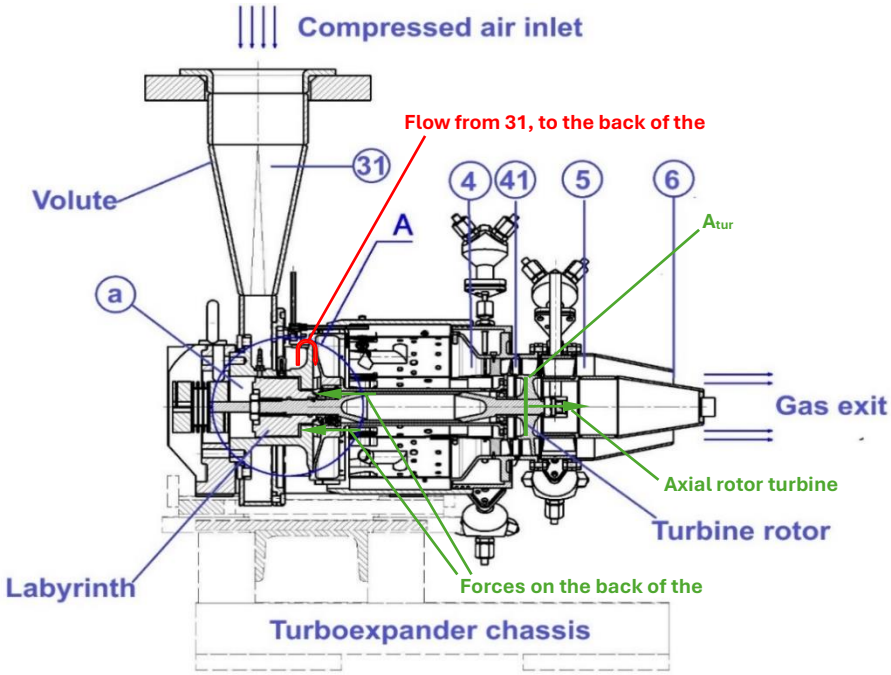

Fig. 2. Turbojet modified for a turboexpander purpose

Figure 2 above, shows the modification of the intake volute, the introduction of an adaptation component in place of the centrifugal compressor rotor and the introduction of the labyrinth thus designed with two shoulders. These are intended to handle the pressure that was theoretically present behind the

centrifugal compressor and to generate a force opposing the axial thrust force of the turbine, which is induced by the back pressure on the aerodynamic forces acting on it. The shoulder of the labyrinth was calculated in such a way as to almost equate the axial force acting on the disk of the rotor turbine (axial rotor turbine thrust), see figure 2.

In table 1 have been presented the data from the preliminary calculation, in which were considered: two sealing stages of the labyrinth, the total pressure behind the axial turbine, the area of the rotor turbine disk A_{turb}, the pressure behind the turbine (denoted as p_{41} in section 41of fig. 2), the total area of those two labyrinth steps given by the two diameters D_1 and D_2, where D_1 is imposed and D_2 will result. Axial force on the labyrinth is:

$$F_{ax\_lab} = A_1 \cdot p_{1_{lab}} + A_2 \cdot p_{2_{lab}} \sim F_{ax\_turb} \quad (1)$$

$$A_2 = \frac{\left(F_{ax_{turb}} - A_1 \cdot p_{1_{lab}}\right)}{p_{2_{lab}}} = \pi/4 \cdot (D_2^2 - D_1^2) \quad (2)$$

Using Eq. 1 and 2, we will determine the diameter D_2. Where $p_{1\_lab} = p_{31} = 4.5 \cdot \xi = 4.4$ bar abs., $\xi = 0.98$ (loss coefficient), the pressure after the first step of the labyrinth $p_{2\_lab} = 3.3$ bar abs (given by the simulation data) and the central diameter of the shaft, d_{ax}, on which the labyrinth is located (see figure 3). The turbine being half active and half reactive, the axial thrust given by the reactive force can be neglected as it is 3 orders of magnitude smaller, and, so, the main axial thrust is given by pressure on the rotor disk area A_{turb}. The $p_{41} = 2.86$ bar abs is the static pressure on the A_{turb} area and is given by the GasTurb 13 [5] calculations.

Table 1. Parameters data in the analysed points

A_{turb} [mm^2]	p_{41} [bar abs]	F_{ax_turb} [N]	p_{1_lab} [bar abs]	Dax [mm]	A_1 [mm^2]	D1 [mm]	p_{2_lab} [bar abs]	D_2 [mm]	A_2 [mm^2]	D'_2 [mm]	A'_2 [mm^2]
3215	2.86	552.8	4.4	14.3	747.3	34	3.3	45	678.7	58.1	1754

Given the technological constraints and potential higher pressures experienced during testing, a larger diameter of approx. D_2'=Ø60mm (with a specific value of Ø58.1, as seen in fig. 3) is used for the labyrinth. The turboexpander being subjected during the tests to higher pressures, there may be greater forces on the turbine disc that should be compensated, the maximum resultant force in normal operation (4.5 bar abs suction) will be:

$$F_{rez} = F_{turb} - F_{ax_{lab(58.1mm)}} = 351.2N\ (79\ lbf) \quad (3)$$

The axial force on the turbine disc, as calculated, is managed by the axial-radial hybrid bearings. The chosen hybrid bearings are of the angular contact type, designed to handle both combined axial and radial loads. These bearings are equipped with ceramic balls to enhance performance and durability [6] and are paired to ensure proper operations.

The total air flow through the turbine is considered at M=0.7 kg/s. The air flow accepted as losses in labyrinth is 2% of the initial flow, namely: $m_{loss} = M \cdot 0.02 = 0.014$kg/s. Figures 3 and 4 illustrate the detailed dimensions of the labyrinth and the specifications of the teeth. The labyrinth calculations have been performed using both analytical and numerical methods to ensure accuracy and reliability.

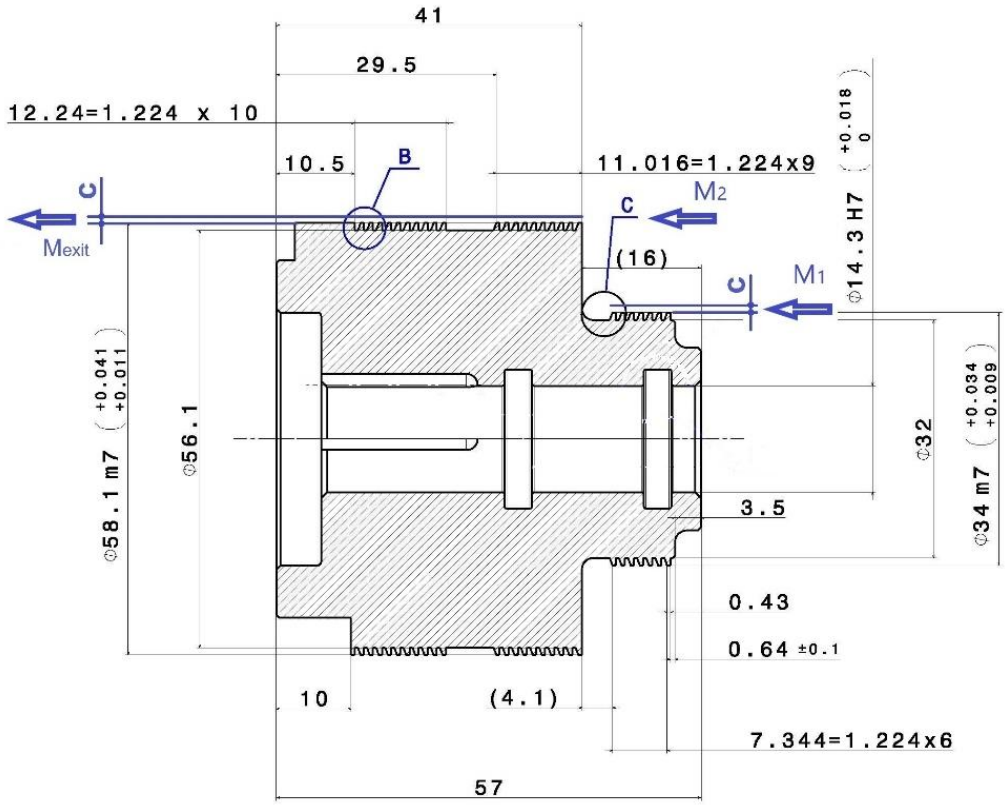

Fig. 3. Labyrinth design

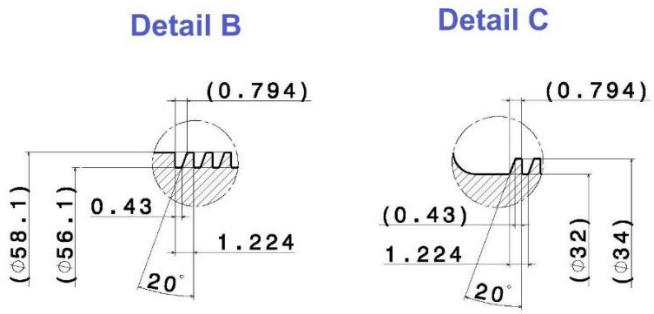

Fig. 4. Details of the labyrinth

The analytical method has been developed based on previous calculations made by P. Kaszowski et al. [7] and D. Joachimiak [8]. In the methods described in [7, 8] the calculations are made by iterations, based on several assumptions:

a. The flow through the teeth is considered isentropic
b. The mass flow through the teeth is constant
c. The total enthalpy is constant, and the fluid loses its energy by being transformed into heat (increasing the enthalpy)

In figure 5 is shown a schematic drawing of the labyrinth [7].

Technium Vol. 24, pp.1-10 (2024)
ISSN: 2668-778X
www.techniumscience.com

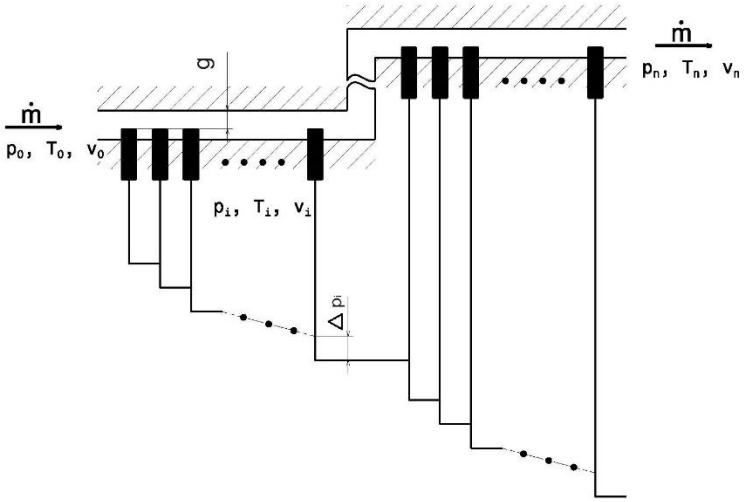

Fig. 5. Scheme of the labyrinth

In figure 6, the Fanno line for a labyrinth seal with a step is shown. From above, the flow through a tooth is considered isentropic, and as is shown in fig. 6, from point 0 to point 1 is a drop of enthalpy given by the equation:

$$\Delta h = \frac{c^2}{2} \tag{4}$$

where c is the velocity of the flow bypassing the gap g of the seal, through the area. For first step:

$$A_{g1} = \frac{\pi}{4}((D_1 + 2 \cdot g)^2 - D_1^2) \tag{5}$$

and for the second step:

$$A_{g2} = \frac{\pi}{4}((D_2 + 2 \cdot g)^2 - D_2^2) \tag{6}$$

The gas velocity at the exit of the seal segment I is given by the equation of continuity:

$$c_i = v_i \cdot \frac{\dot{m}_i}{A_i} \tag{7}$$

where $\dot{m}_i$, A_i , v_i are the mass flow rate, area and specific volume in the point i, respectively.

From figure 6, the gas undergoes an isobaric transformation from point 1 to point 1'. During this transformation the kinetic energy given by the velocity c is converted into heat and added to the enthalpy. The enthalpy in the point 1' will be:

$$h_1' = h_1 + \Delta h = h_0 \tag{8}$$

Technium Vol. 24, pp.1-10 (2024)
ISSN: 2668-778X
www.techniumscience.com

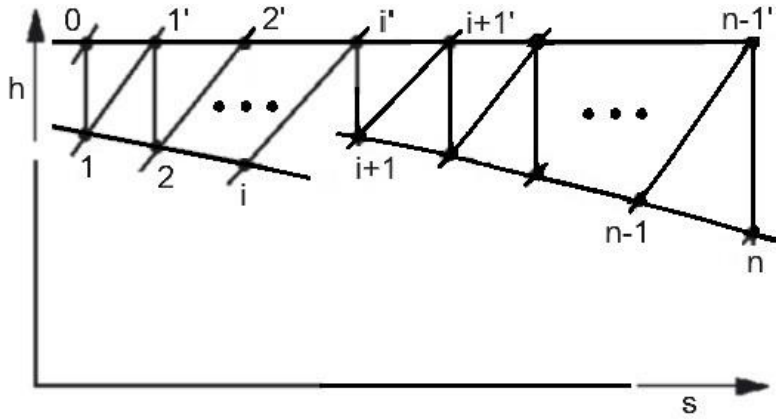

Fig. 6. Fanno line for two step seal with $h_{i+1}>h_i$

Finding the thermodynamic parameters in the points 1…n-1, it is assumed that the specific gas constant R and specific heat capacity at constant pressure c_p are constant values. As the pressure will decrease along the teeth of the labyrinth, the density of the gas will also decrease (the specific volume will do the opposite), the velocity of the gas will increase along the labyrinth teeth. The enthalpy in point 0 had been obtained from the thermodynamic tables [9]. The total temperature in the point 1'…n-1' will increase slightly, given by the reduction of the gas flow. The total temperature is given by the equations:

$$T_i' = T_i \cdot \left(1 + \left(\frac{k-1}{2}\right) \cdot {M_i}^2\right) \tag{9}$$

$$M_i = \frac{c_i}{a_i}; \qquad c_i = f(m_i, A_i, v_i); \qquad a_i = \sqrt{k \cdot p_i \cdot v_i} \tag{10}$$

$$v_i = v_{i-1} \cdot \frac{p_{i-1} \cdot T_i}{p_i \cdot T_{i-1}} \tag{11}$$

$$v_i' = v_{i-1}' \cdot \frac{p_{i-1} \cdot T_i'}{p_i \cdot T_{i-1}'} \tag{12}$$

$$T_i = T_{i-1} - \frac{\Delta h_i}{c_p} \tag{13}$$

$$m_i = A_i \cdot \sqrt{2 \cdot \frac{k}{k-1} \cdot \frac{p_{i-1}}{v_{i-1}} \cdot \left[\left(\frac{p_i}{p_{i-1}}\right)^{\frac{2}{k}} - \left(\frac{p_i}{p_{i-1}}\right)^{\frac{k-1}{k}}\right]} \tag{14}$$

where, $c_p = 1003.4\ \frac{J}{kg \cdot K}$, and $R = 286.7 \frac{J}{kg \cdot K}$. T_0=50°C=323.16K. T_i is the static temperature in the point i, v_i is the static specific volume in the point i, T_i' is the total temperature in the point i', and v_i' is the total specific volume in the point i'. $p_i' = p_i$ (total pressure will become static pressure between the labyrinth teeth). The total number of teeth considered is 28 and the number of spaces between them is 26. The step is between the teeth no. 7 and 8, where is a step of the area from A_{1g} to A_{2g}, from diameter D_1=34 mm to D_2=58.1 mm. For iterations, the difference pressure from the entry and the exit of the labyrinth is divided to the number of spaces between teeth. The initial pressure gap will be:

$$\Delta p_i = \frac{p_0}{p_n \cdot 26} = \frac{p_{31} \cdot \xi}{p_{atm}} = 0.13026 \tag{15}$$

where: p_{atm} = 101,325 N/m^2.

As the mass flow through the teeth is a non-linear function of p_i, some corrections have been introduced using the differentials of the mass flow function of p_i and p_{i+1} [7, 8]. The equation (14) is developed into Taylor series, keeping the first derivative and so is obtained the equation:

$$d\dot{m}_i = \frac{\partial \dot{m}_i}{\partial p_{i-1}} dp_{i-1} + \frac{\partial \dot{m}_i}{\partial p_i} dp_i \tag{16}$$

That can make possible the determination of pressure corrections Δp_1, $\Delta p_2 \ldots \Delta p_{27}$.
The partial derivatives (using Mathcad symbolic evaluation operator) from equation (16) are:

$$\frac{\partial \dot{m}_i}{\partial p_{i-1}} = \frac{A_i \cdot \left[\left(\frac{p_i}{p_{i-1}} \right)^{\frac{2}{k}} \cdot (k-2) + \left(\frac{p_i}{p_{i-1}} \right)^{\frac{k+1}{k}} \right]}{\sqrt{2 \cdot p_{i-1} \cdot v_{i-1} \cdot k \cdot \left[\left(\frac{p_i}{p_{i-1}} \right)^{\frac{2}{k}} - \left(\frac{p_i}{p_{i-1}} \right)^{\frac{k+1}{k}} \right]}} \tag{17}$$

and,

$$\frac{\partial \dot{m}_i}{\partial p_i} = \frac{A_i \cdot \left[\left(\frac{p_i}{p_{i-1}} \right)^{\frac{2-k}{k}} - \frac{k+1}{k} \cdot \left(\frac{p_i}{p_{i-1}} \right)^{\frac{1}{k}} \right]}{\sqrt{p_{i-1} \cdot v_{i-1} \cdot \frac{k-1}{2} \cdot \left[\left(\frac{p_i}{p_{i-1}} \right)^{\frac{2}{k}} - \left(\frac{p_i}{p_{i-1}} \right)^{\frac{k+1}{k}} \right]}} \tag{18}$$

Assuming that Δp_i and Δm_i are small enough, the equation (16) will become:

$$\Delta\dot{m}_i = \frac{\partial \dot{m}_i}{\partial p_{i-1}} \Delta p_{i-1} + \frac{\partial \dot{m}_i}{\partial p_i} \Delta p_i \tag{19}$$

and will end up with 27 equations for 27 Δp_i unknowns:

$$\begin{aligned} \Delta\dot{m}_1 &= \frac{\partial \dot{m}_1}{\partial p_0} \Delta p_0 + \frac{\partial \dot{m}_1}{\partial p_1} \Delta p_1 \\ \Delta\dot{m}_2 &= \frac{\partial \dot{m}_2}{\partial p_1} \Delta p_1 + \frac{\partial \dot{m}_2}{\partial p_2} \Delta p_2 \\ &\ldots \\ \Delta\dot{m}_{n-1} &= \frac{\partial \dot{m}_{n-1}}{\partial p_{n-2}} \Delta p_{n-2} + \frac{\partial \dot{m}_{n-1}}{\partial p_{n-1}} \Delta p_{n-1} \end{aligned} \tag{20}$$

also,

$$\begin{aligned} \Delta\dot{m}_1 &= \dot{m}_1 - \dot{m}_2 \\ &\ldots \\ \Delta\dot{m}_{n-1} &= \dot{m}_{n-1} - \dot{m}_n \end{aligned} \tag{21}$$

The system of 27 equations with 27 unknowns can be resolved using a matrix system:

$$A \cdot X = B \tag{22}$$

where:

Technium Vol. 24, pp.1-10 (2024)
ISSN: 2668-778X
www.techniumscience.com

$$A = \begin{bmatrix} \frac{\partial \dot{m}_1}{\partial p_1} & 0 & \cdots & 0 & 0 & 0 \\ \frac{\partial \dot{m}_2}{\partial p_1} & \frac{\partial \dot{m}_2}{\partial p_2} & \cdots & 0 & 0 & 0 \\ \vdots & \frac{\partial \dot{m}_3}{\partial p_2} & \frac{\partial \dot{m}_3}{\partial p_3} & \cdots & 0 & 0 \\ 0 & \vdots & \vdots & \ddots & 0 & 0 \\ 0 & 0 & \cdots & \frac{\partial \dot{m}_{n-2}}{\partial p_{n-3}} & \frac{\partial \dot{m}_{n-2}}{\partial p_{n-2}} & \vdots \\ 0 & 0 & 0 & \cdots & \frac{\partial \dot{m}_{n-1}}{\partial p_{n-2}} & \frac{\partial \dot{m}_{n-1}}{\partial p_{n-1}} \end{bmatrix}; \quad X = \begin{bmatrix} \Delta p_1 \\ \vdots \\ \Delta p_{n-1} \end{bmatrix}; \quad B = \begin{bmatrix} \dot{m}_1 - \dot{m}_2 \\ \vdots \\ \dot{m}_{n-1} - \dot{m}_n \end{bmatrix}; \tag{23}$$

The solution is given by inversing the matrix A:

$$X = A^{-1} \cdot B \tag{24}$$

The calculated Δp_i values were incorporated into the existing values using the relation from Eq. 15. This process was iterated until the solution converged with an error margin of 0.1 %. During this iterative procedure, the static temperature of the labyrinth exit was observed to decrease by approximately 4.5°C, excluding the effects of heat transfer.

The following curve has been obtained in the figure 7, for the pressure drop along the labyrinth:

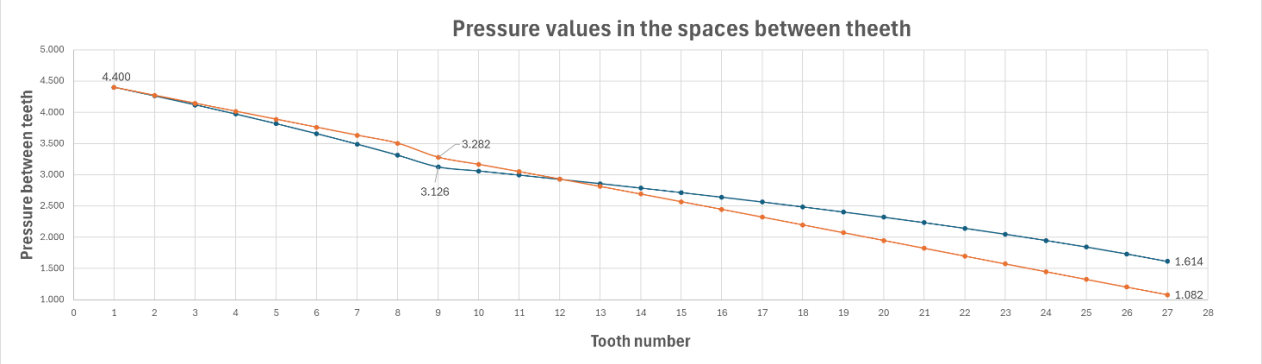

Fig. 7. Pressure variation along the labyrinth teeth

It is observed an inflexion between teeth 8 and 9, that is given by the changing of the area from A_{1_gap} = 2.65072E-05 mm^2 to A_{2_gap} = 4.54353E-05 mm^2, in the context of increasing it, this involves altering the velocity of the flow, and the observing how the pressure changes, all while maintaining a constant mass flow.

In figure 8 it is observed a very small variation in the mass flow rate around the medium value:

$$\dot{m}_{medium} = 0.00935 \text{ kg/s}. \tag{25}$$

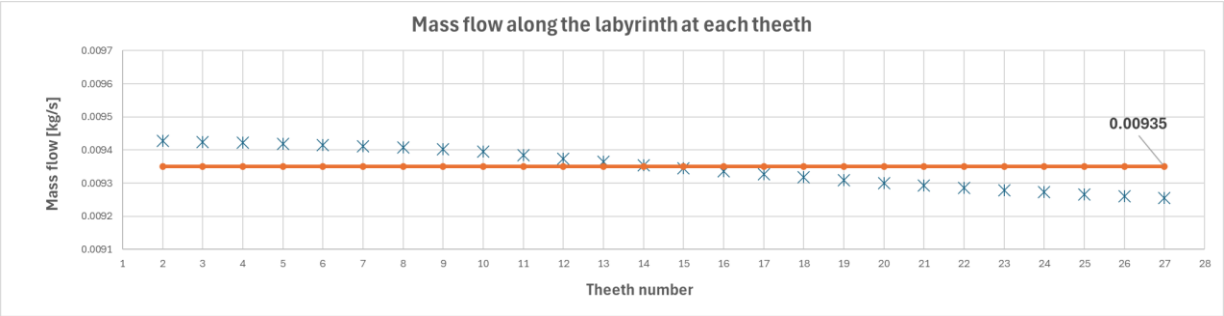

Fig. 8. Mass flow variation along the labyrinth teeth

Technium Vol. 24, pp.1-10 (2024)
ISSN: 2668-778X
www.techniumscience.com

In figure 7 it is observed that the pressure in point 27 is increased to the value p_{27}=1.614 bar, that can be explained by an extra flow over the existing one. If it is supposed an expansion from p_{27} to p_{atm}, using an area $A_{2\_gap\_corrected} = A_{2\_gap} \cdot \zeta = 3.56667E\text{-}05$, where ζ =0.785 is the flow correction coefficient [10], an extra flow using the Eq. 14 with the value from point 27, is found:

$$\dot{m}_{extra} = 0.01266 kg/s \tag{26}$$

The total flow supposed to bypass the labyrinth will be:

$$\dot{m}_{total} = \dot{m}_{extra} + \dot{m}_{medium} = 0.0221\ kg/s \tag{27}$$

and that is about 3.15% from the 0.7 kg/s flow through turbine, and almost 1.5 times the desired value of 2% losses. The Fanno line for two-stage labyrinth is presented in the figure below.

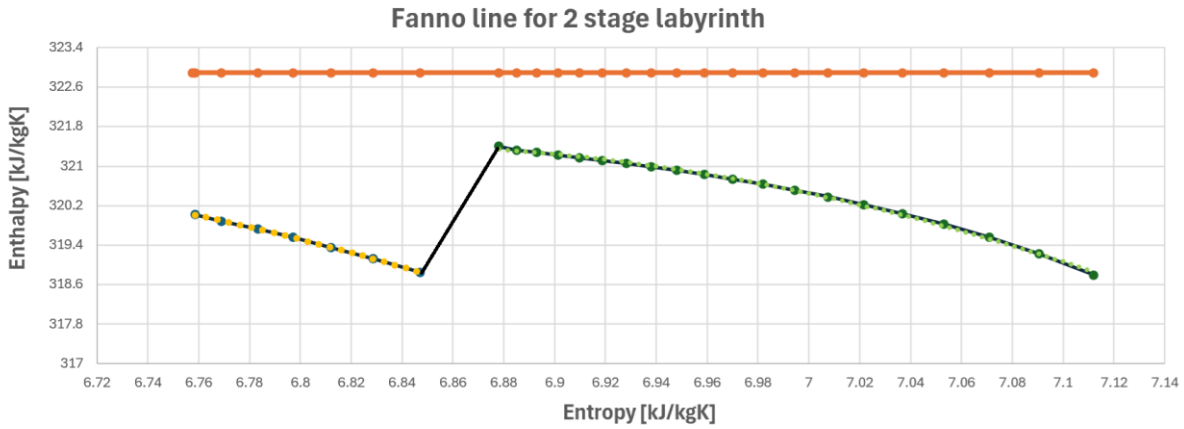

Fig. 9. Fanno line for two stage labyrinth

In figure 10, the results from the numerical analysis are presented. The analysis shows a value for mass flow of 0.016 kg/s, which represents 2.3% losses from the initial 0.7 kg/s turbine flow.

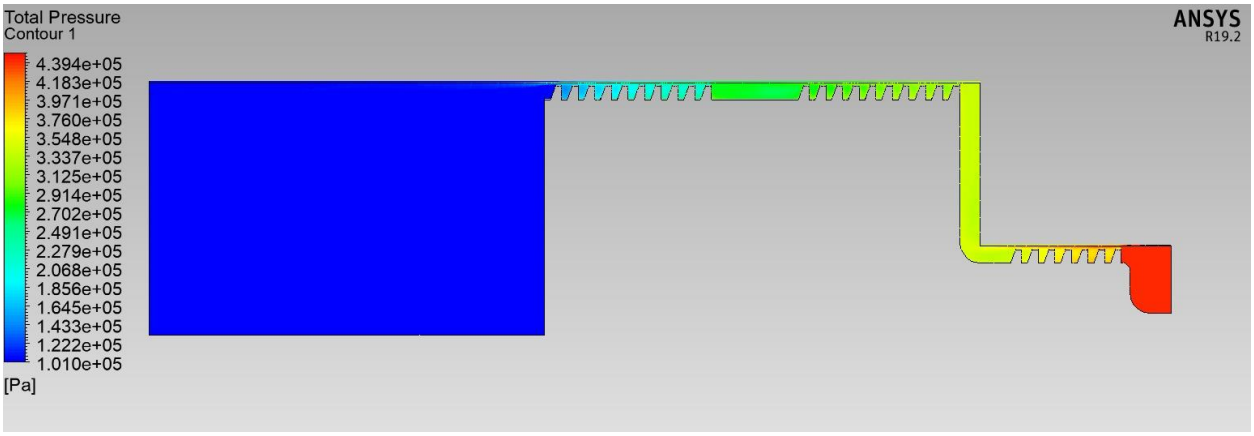

Fig. 10. Total pressure distribution in numerical analysis

The error in the analitical method is greater from the numerical one, but the method gives a fairly good approximation to the real flow in the labyrinth.

3. Conclusions

The presented method is new in terms of the iterative determination of the flow parameters through a two-step labyrinth, based on calculation methodologies existing in the specialized literature [7, 8].

The work analyzes the phenomenon at an intermediate, analytical level, which does not give sufficiently good accuracy regarding the final result, but it can determine the magnitude of the fluid lost through the labyrinth thus pre-designed. There were not taken into consideration the heat transfer and, also, the influence of the rotational speed, where other specialized works have been done, where a decreasing of the leakage with the increasing of the rotational speed has been observed [11]. Also, has been not taken into consideration the form of the teeth. A comparison was made with a finite element calculation and the conclusion was that the results are comparable in the assumptions done. The calculation error in determining the enthalpies of about 0.5% is given by the consideration of the specific gas constant R and specific heat capacity at constant pressure c_P at constant values as for an ideal fluid. The entropies have been calculated from the thermodynamic tables [9], where a 4 points Lagrange interpolation has been done. The final graph from the figure 9, shows the Fanno line, made in h-s coordinate [11], for the presented labyrinth for a subsonic leakage flow, with Mach numbers < 0.25 in the present work and with a Reynolds number < 11500. The flow losses in the presented paper are over the desired ones, in an amount of 1.5 times the 2% leakage desired, but in the numerical analysis the loss leakage is about 2.3%, which is close to the desired losses. The high rotational speed limits the current 0.25 mm gap at the tip of the teeth, as high vibration have been observed during labyrinth operation, and as consequence, further investigations must be carried out regarding the materials used and vibration reduction techniques to reduce the gap between the teeth of the labyrinth and the cylinder in which it rotates.

Acknowledgements

"This work was carried out through the "NUCLEU" Programme within the National Research Development and Innovation Plan 2022-2027, carried out with the support of MCID, project no. PN23.12.01.01".

References

[1] JetCat P400-PRO-LN, Ingenieurbüro CAT, M. *Zipperer GmbH*. Available online: https://www.jetcat.de/en/productdetails/produkte/jetcat/produkte/Professionell/p400%20pro

[2] Turboexpander, Encyclopedia of Marine and Energy Technology, *Wärtsilä Corporation*, Finland. Available online: https://www.wartsila.com/encyclopedia/term/turboexpander

[3] J. LARGE, A. PESYRIDIS, Investigation of Micro Gas Turbine Systems for High Speed Long Loiter Tactical Unmanned Air Systems, *Aerospace* 6 (5), 55, 2019; https://doi.org/10.3390/aerospace6050055

[4] O. DUMITRESCU, V. DRAGAN, B. GHERMAN, Aerodynamic development of a high-pressure ratio compressor for an advanced microturbine powerplant, *IOP Conf. Series: Materials Science and Engineering* **916,** 012034, 2020, doi:10.1088/1757-899X/916/1/012034

[5] GasTurb 13, Design and Off-Design Performance of Gas Turbines, *GasTurb GmbH*. Available online: https://www.gasturb.com/Downloads/Manuals/GasTurb13.pdf

[6] Spindle ball bearing HY SM 6002 C TA P4+. Available online: https://www.gmn.de/?ddf=1&t=kugellager&i=176&c=257101423251732290&l=en

[7] P. KASZOWSKI, M. DZIDA, P. KRZYŚLAK, Calculations of labyrinth seals with and without diagnostic extraction in fluid-flow machines, *Polish Maritime Research*, **20**, 4 (80), pp. 34-38, 2013, https://doi.org/10.2478/pomr-2013-0038

[8] D. JOACHIMIAK, Universal Method for Determination of Leakage in Labyrinth Seal, Journal of Applied Fluid Mechanics, **13**, 3, pp. 935-943, 2020, https://doi.org/10.29252/jafm.13.03.30618

[9] J. HILSENRATH, C. W. BECKETT, W. S. BENEDICT, L. FANO, H. J. HOGE, J. F. MASI, R. L. NUTTALL, Y. S. TOULOUKIAN, H. W. WOOLLEY, C. V. KING, Tables of Thermal Properties of Gases, *National Bureau of Standards Circular 564*, 1956. Available online: https://nvlpubs.nist.gov/nistpubs/Legacy/circ/nbscircular564.pdf

[10] Vs. RADCENCO, N. ALEXANDRESCU, E. IONESCU, M. IONESCU, Calculul şi proiectarea elementelor şi schemelor pneumatice de automatizare (Computation and Design of Pneumatic Automation Elements and Diagrams), *Editura Tehnică*, Bucureşti, 1985.

[11] Z. WANG, B. ZHANG, Y. CHEN, S. YANG, H. LIU, H. JI, Investigation of Leakage and Heat Transfer Properties of the Labyrinth Seal on Various Rotation Speed and Geometric Parameters, *Coatings*, **12**, 586, 2022, https://doi.org/10.3390/coatings12050586

[12] S. A. SAINCHER, Lecture 3 Fanno Flow, *Author Content*, 2019 http://dx.doi.org/10.13140/RG.2.2.36198.98886